Landslides (2017) 14:35–45
DOI 10.1007/s10346-016-0692-8
Received: 18 April 2015
Accepted: 24 February 2016
Published online: 16 March 2016

Enrico Conte · Antonio Donato · Antonello Troncone

A simplified method for predicting rainfall-induced mobility of active landslides

Abstract This paper deals with the landslides that are reactivated by a groundwater level increase owing to rainfall. These landslides are usually characterized by low displacement rate with deformations essentially concentrated within a narrow shear zone above which the unstable soil mass moves like a rigid body (i.e., with a horizontal displacement profile that is essentially constant with depth). In view of this evidence, a new method based on a simple sliding block model is proposed in the present study for a preliminary evaluation of landslide mobility. Unlike other existing methods that provide an evaluation of landslide mobility on the basis of groundwater level measurements, the present method directly relates landslide movements to rain recordings. This possibility constitutes a significant advantage from a practical viewpoint because it allows future displacement scenarios to be predicted from expected rainfall scenarios. In addition, the present method requires a limited number of parameters as input data, many of which can be obtained from conventional geotechnical tests. To evaluate the other parameters involved, an efficient calibration procedure is also proposed. Four case studies documented in the literature are analyzed to assess the capability of the present method to reproduce the main features of the slope response to rainfall. In all these case studies, both groundwater level variations and landslide displacements observed in field are well approximated by the method.

Keywords Rainfall · Groundwater level fluctuations · Landslide mobility · Sliding block model

Introduction

Active landslides are often controlled by the groundwater level fluctuations which in turn are related to rainfall. The mobility of these landslides is therefore characterized by alternating phases of rest and motion according to the weather conditions. In particular, a rising groundwater level owing to rainfall can cause a reactivation of the landslide or, if it is moving, an acceleration of the motion. On the other hand, a groundwater level lowering (as it occurs during dry periods) reduces the landslide velocity and can bring the unstable soil mass to rest. The main type of movement experienced by these landslides is a translational slide with a velocity in the order of some centimeters per year, so that they can be defined as slow-moving landslides (Cruden and Varnes 1996). Generally, soil deformations are concentrated within a narrow shear zone located at the base of the landslide body, in which the soil shear strength is at residual condition owing to the high strains accumulated (Leroueil et al. 1996). The soil above the shear zone is, on the contrary, affected by small strains and it is often characterized by a horizontal displacement profile that is essentially constant with depth.

In engineering practice, changes in the groundwater regime and slope stability are usually dealt with separately using an uncoupled approach. Specifically, the pore water pressure regime within the slope due to groundwater level variations is first determined. Then, the resulting pore water pressures at the potential failure surface are used in a limit equilibrium analysis for assessing the slope stability conditions in terms of a safety factor defined as the ratio of the soil shear strength available along the failure surface to that mobilized. In this context, Van Asch and Buma (1997) proposed a one-dimensional hydrological model to describe groundwater fluctuations in relation to precipitation and a limit equilibrium method to assess the temporal frequency of instability of a landslide. Conte and Troncone (2012a) developed a simplified method that utilizes the infinite slope model to assess slope stability and an analytical solution (Conte and Troncone 2008) to evaluate the changes in pore pressure at the slip surface from the piezometric measurements carried out at a piezometer installed above this surface. However, the limit equilibrium method is in principle unable to analyze active landslides for which a realistic prediction of the displacements is required rather than a calculation of the safety factor. Owing to this drawback, Calvello et al. (2008) proposed to relate empirically the displacement rate measured at a selected point of the slope to the safety factor value calculated using the limit equilibrium method.

Numerical solutions based on the finite element method or the finite difference method can obviously provide a better understanding of the complex mechanisms of deformation that occur in the slopes (Di Maio et al. 2010; Lollino et al. 2010; Vassallo et al. 2015). Considering that in the slow-moving landslides, the viscous component of the soil deformations should be very important (Vulliet and Hutter 1988; Van Asch and Van Genuchten 1990; Bracegirdle et al. 1992; Savage and Chleborad 1982; Desai et al. 1995; Van Asch et al. 2007), an elasto-viscoplastic constitutive model is often incorporated in these numerical methods to predict the behavior of the unstable soil mass (Olivella et al. 1996; Picarelli et al. 2004; Fernández-Merodo et al. 2014). Recently, Conte et al. (2014) presented a finite element approach for evaluating the mobility of active landslides owing to groundwater level fluctuations. This approach utilizes an elasto-viscoplastic constitutive model in conjunction with a Mohr-Coulomb yield function to model the behavior of the soil in the shear zone. A linear elastic model is on the contrary assumed for the soils above the shear zone which, as already said, undergo small strains. However, the numerical methods are generally very costly from a computational viewpoint. In addition, a significant number of material parameters need to be evaluated when advanced constitutive models are adopted. As a consequence, the use of these methods is not fully justified for practical purposes especially when there is a lack of precise measurements or specific experimental data concerning the constitutive parameters involved.

Simplified methods that are based on approximate assumptions were also proposed to perform readily a preliminary assessment of the landslide mobility (Hutchinson 1986; Angeli et al. 1996; Gottardi and Butterfield 2001; Corominas et al. 2005; Herrera et al. 2009; Ranalli et al. 2010; Conte and Troncone 2011, 2012c). Specifically, in these methods it is assumed that the

landslide body behaves as a rigid block sliding on an inclined plane. The resulting solution is generally simple to use and is not time-consuming. Another significant advantage lies in the fact that few material parameters are required as input data, most of which can be obtained by conventional geotechnical tests. In these methods, however, landslide velocity is usually evaluated on the basis of the groundwater level measurements carried out at some piezometers installed within the slope. This constitutes a serious drawback when such methods are used as a predictive tool to evaluate the landslide movements from expected rainfall scenarios, because the associated groundwater level changes are not known. As a consequence, a method that directly relates rainfall to landslide mobility should be of major interest from a practical viewpoint. A method with these characteristics is developed in the present study. This method utilizes some analytical solutions which relate rainfall to groundwater level changes and the latter to the landslide movements. A calibration procedure is also incorporated in the method to evaluate some parameters which are difficult to obtain experimentally. Several case studies documented in the literature are considered to assess the capability of the proposed method to predict the landslide mobility caused by rainfall.

Proposed method

Relationship between rainfall and groundwater level variations

Novel equations are derived in this section to establish a simple relationship between rainfall and groundwater level fluctuations. To this end, the scheme shown in Fig. 1 is considered. It concerns an infinite slope that makes an angle α with the horizontal direction and is subjected to water seepage parallel to the ground surface. Referring to Fig. 1, H is the thickness of the landslide body, H_d is the depth of the steady-state groundwater level from the ground surface, H_w is the distance between the steady-state level and the slip surface and $h(t)$ denotes the change in the groundwater level caused by rain infiltration. All these quantities are measured in the vertical direction (Fig. 1).

Owing to the occurrence of continuous movements, the upper portion of the landslide body is generally characterized by the presence of cracks and fissures which favor water infiltration into the slope (Van Asch et al. 1996), with the result that a close relationship is often observed between rainfall and groundwater level fluctuations. This also occurs in low permeable soils where the rainfall-groundwater level relationship is generally more complex. Under the assumption of a perfect synchronism between rainfall and groundwater fluctuations, the following equation can be written:

$$h_r = n\,(1-S_r)\,h_o \tag{1a}$$

where h_r is the water volume (per unit area) that infiltrates into the slope owing to a rain event with a prescribed duration, h_o is the corresponding increase in groundwater level with respect to the steady-state level, and n and S_r are, respectively, the porosity and degree of saturation in the portion of soil above the steady-state groundwater level. The term $n\,(1-S_r)\,h_o$ is therefore the water volume (per unit area) that is stored into the soil owing to infiltration. As a further simplification, it is assumed that both n and S_r are constant. Of course, when the slope is completely saturated ($S_r = 1$), rain cannot infiltrate through the ground surface and therefore $h_r = 0$. Equation (1a) can be also written as

$$h_o = \frac{h_r}{n\,(1-S_r)} \text{ with } S_r < 1 \tag{1b}$$

It is also noteworthy that $h_o \le H_d$ in this equation. To account for approximately the runoff effect, it is assumed that h_r is related to the rain depth, h_m, by an expression similar to that suggested by Conte and Troncone (2012b), i.e.,

$$h_r = h_m \text{ for } h_m < \overline{h} \tag{2a}$$

$$h_r = \overline{h} \text{ for } h_m \ge \overline{h} \tag{2b}$$

where $\overline{h}$ is the potential infiltration volume (per unit area) through the ground surface (Fig. 2). A constant value of $\overline{h}$ is considered in the present study, for the sake of simplicity.

The water volume stored in the soil progressively reduces in consequence of the water seepage that occurs in the saturated portion of the slope. Considering a slope slice with unit width, b, the following balance equation can be written in differential form:

$$-dh\,b = k\,i\,h\cos\alpha\,dt \tag{3}$$

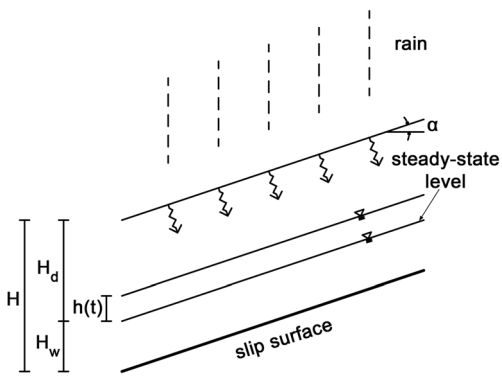

Fig. 1 Infinite slope model with an indication of the steady-state groundwater level, the groundwater level change owing to rain infiltration, $h(t)$, and the slip surface (modified from Conte and Troncone 2011)

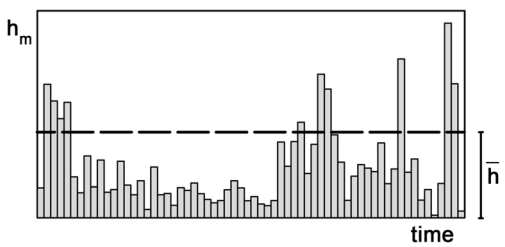

Fig. 2 Rain depth, h_m, and potential rain infiltration depth, $\overline{h}$

where t is time, k is the saturated hydraulic conductivity of the soil, and i is the hydraulic gradient ($i = \sin\alpha$ for an infinite slope with water flow parallel to the slope). Setting $k_T = k/b$, Eq. (3) takes the form

$$\frac{dh}{h} = -k_T \sin\alpha \cos\alpha \, dt \tag{4}$$

Integrating this equation with the initial condition $h = h_o$ at $t = t_o$, and taking into account Eq. (1a), leads to the following solution for $h(t)$:

$$h(t) = \frac{h_r}{n\,(1-S_r)} \exp\left[-k_T \sin\alpha \cos\alpha \quad (t-t_o)\right] \tag{5}$$

It can be readily extended to a number N of rain events using the equation

$$h(t) = \sum_{j=1}^{N} \frac{h_{rj}}{n\,(1-S_r)} \exp\left[-k_T \sin\alpha \cos\alpha \quad \left(t-t_{oj}\right)\right] \tag{6}$$

where h_{r_j} is the water volume (per unit area) that infiltrates into the slope owing to the *j-th* rain event. An equation similar to Eq. (6) was derived by Montrasio and Valentino (2007, 2008) to study a different problem (i.e., the triggering mechanism of rainfall-induced shallow landslides).

Finally, the changes in pore water pressure associated with $h(t)$ are given by

$$u_o(t) = \gamma_w h(t) \cos^2\alpha \tag{7}$$

where γ_w is the unit weight of water.

Prediction of landslide mobility

In this section, the method originally proposed by Conte and Troncone (2011) is extended to evaluate the landslide movements using the function $u_o(t)$ which is directly related to rain infiltration by Eqs. (6) and (7). In this method, the infinite slope model shown in Fig. 3 is considered, where d is the thickness of the shear zone above which the unstable soil mass moves like a rigid body. It is also assumed that a viscous force is activated at the base of the landslide body when movement occurs. Under these assumptions, the equation of motion takes the form

$$\frac{dv}{dt} + \lambda v = \chi\left[u(t) - u_c\right] \tag{8}$$

where $v(t)$ is the landslide velocity in the direction parallel to the slope, $u(t)$ describes the changes in pore water pressure at the failure surface, and u_c is a critical threshold for $u(t)$, which is introduced to establish whether or not the landslide body moves. Specifically, motion occurs when $u(t)$ exceeds u_c. The expression of u_c is

$$u_c = \frac{1}{\tan\phi_r'}\left(c_r' - \gamma H \sin\alpha\cos\alpha\right) + \left(\gamma H - \gamma_w H_w\right)\cos^2\alpha \tag{9}$$

in which γ is the unit weight of the soil which is assumed constant with depth for simplicity, c_r' and ϕ_r' are, respectively, the effective cohesion and the resistance angle of the soil (in the shear zone) at residual condition. The other parameters appearing in Eq. (8) are

$$\lambda = \frac{\beta}{\gamma H} g \tag{10}$$

$$\beta = \frac{\mu}{d} \tag{11}$$

$$\chi = \frac{\tan\phi_r'}{\gamma H \cos\alpha} g \tag{12}$$

with μ = coefficient of viscosity of the soil in the shear zone and g = gravity acceleration.

After expanding the function $u_o(t)$ in a finite number M of harmonic components using the Fourier series, i.e.,

$$u_o(t) = \frac{A_o}{2} + \sum_{k=1}^{M} \left[A_k \cos\left(\omega_k t\right) + B_k \sin\left(\omega_k t\right)\right] \tag{13}$$

where $\omega_k = 2k\pi/T$ is the frequency of the k^{th} component, T is the period of $u_o(t)$ which has to be assumed greater than the final time of analysis, and A_o, A_k, and B_k are the series amplitudes, the solution to Eq. (8) can be put in the following form (Conte and Troncone 2011):

$$v(t) = \chi\left\{v_1(t) - v_2(t) + \sum_{k=1}^{M} v_k(t)\right\} \tag{14}$$

where

$$v_1(t) = \frac{A_o}{2}\left\{\frac{1}{\lambda}\left[1 - e^{-\lambda\left(t-t_s\right)}\right] \quad -\frac{4}{\pi}\sum_{n=1}^{\infty} \quad \frac{1}{(2n-1)} \quad \frac{L_n}{S_n} \quad \sin M_n\right\} \tag{15}$$

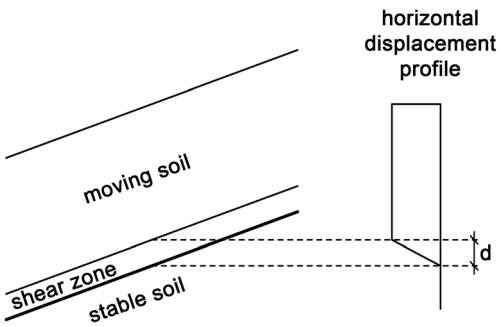

Fig. 3 Slope model considered in the present study (modified from Conte and Troncone 2011)

$$v_2(t) = \frac{u_c}{\lambda}\left[1 - e^{-\lambda(t-t_s)}\right] \tag{16}$$

$$v_k(t) = 2\sum_{n=1}^{\infty} \frac{M_n \vartheta_k}{\left(1 + \vartheta_k^2 M_n^4\right)} \left[G_n - F_n + E_n\right] \sin M_n \tag{17}$$

and t_s is time at which the landslide motion starts (at this time $u = u_c$). In addition,

$$M_n = \frac{(2n-1)\pi}{2} \tag{18}$$

$$L_n = e^{-M_n^2 T_v} - e^{\left[-M_n^2 T_{vs} + \lambda(t_s - t)\right]} \tag{19}$$

$$S_n = \lambda - \frac{M_n^2 c_v}{\left(H_w \cos\alpha\right)^2} \tag{20}$$

$$T_v = \frac{c_v t}{\left(H_w \cos\alpha\right)^2} \tag{21}$$

$$T_{vs} = \frac{c_v t_s}{\left(H_w \cos\alpha\right)^2} \tag{22}$$

$$\vartheta_k = \frac{c_v}{\omega_k \left(H_w \cos\alpha\right)^2} \tag{23}$$

$$G_n = \frac{L_n}{S_n}\left(B_k - A_k \vartheta_k M_n^2\right) \tag{24}$$

$$F_n = C\left(B_k - A_k \vartheta_k M_n^2\right) \tag{25}$$

$$E_n = D\left(A_k + B_k \vartheta_k M_n^2\right) \tag{26}$$

$$C = \frac{1}{\left(\lambda^2 + \omega_k^2\right)}\left\{\lambda\cos(\omega_k t) + \omega_k \sin(\omega_k t) - \left[\lambda\cos(\omega_k t_s) + \omega_k \sin(\omega_k t_s)\right] e^{-\lambda(t-t_s)}\right\} \tag{27}$$

$$D = \frac{1}{\left(\lambda^2 + \omega_k^2\right)}\left\{\lambda\sin(\omega_k t) - \omega_k \cos(\omega_k t) - \left[\lambda\sin(\omega_k t_s) - \omega_k \cos(\omega_k t_s)\right] e^{-\lambda(t-t_s)}\right\} \tag{28}$$

The expression of c_v is

$$c_v = \frac{k}{\gamma_w m_v} \tag{29}$$

where m_v is the coefficient of volume change of the soil skeleton.

Velocity $v(t)$ has to be calculated when $u(t) > u_c$. Motion stops when $v = 0$. By contrast, if the condition $u(t) < u_c$ persists at any time, no movement occurs.

In conclusion, Eqs. (14) to (29) allow the landslide velocity to be evaluated directly from the rain recordings (Eqs. 7 and 13). Landslide mobility in terms of permanent displacement, $s(t)$, is obtained by integration of $v(t)$ in the time intervals in which this function takes positive values (i.e., only the displacements in the downhill direction are calculated).

Calibration procedure

The proposed method requires few soil parameters as input data, most of which can be obtained from conventional geotechnical tests. The latter are γ, ϕ_r', c_r' (generally, c_r' is nil), c_v, n, and S_r. On the contrary, the parameters $\overline{h}$, k_T, and β are difficult to determine experimentally. Operative values of these parameters can be evaluated by matching the available measurements concerning the groundwater level variations, $h(t)$, and the landslide displacement, $s(t)$, with the theoretical results obtained using the present method. In some circumstances, a calibration of c_v and S_r could be also opportune, considering that c_v is significantly affected by the presence of fissures, discontinuities, or thin layers of very permeable materials, and S_r strongly depends on suction.

In the present study, calibration of the abovementioned parameters is achieved by minimizing an objective function defined as the sum of the square of the residuals (i.e., the difference between observation and prediction at any time):

$$S_{obj} = \sum_{i=1}^{m}\left(y_i - \overline{y}_i\right)^2 \tag{30}$$

where S_{obj} indicates the objective function, m is the number of available observations, y_i is the *i-th* component of the observation record, and $\overline{y}_i$ is the corresponding computed value. Specifically, to evaluate the optimal values of $\overline{h}$, k_T, n, and S_r (or directly the term $n(1 - S_r)$ appearing in Eq. 6), y_i and $\overline{y}_i$ are the observed and predicted changes in the groundwater level, respectively. Similarly, the measured and calculated values of $s(t)$ are used as y_i and $\overline{y}_i$ to calibrate the parameters c_v and β. The minimization process of S_{obj} is performed using the trust region reflective algorithm (MathWorks 2012). This algorithm is a subspace trust region method and is based on the interior-reflective Newton method described in Coleman and Li (1994, 1996). The trust region method generates a series of intermediate steps with the help of a quadratic model of the objective function. The method selects the direction and size of the step simultaneously. If a step is not acceptable, the size of the region is reduced and a new minimum is found. In general, the direction of the step changes whenever the size of the trust region is altered. Each iteration involves the solution of a linear system of equations using the method of the preconditioned

conjugate gradients. A detailed description of the theory and implementation of the method can be found in MathWorks (2012).

Application of the method to case studies

The proposed method is implemented in a MatLab code which is used in this section to analyze some case studies documented in the literature. In particular, four case studies are considered: the Fosso San Martino landslide (Bertini et al. 1984) and the Orvieto landslide (Tommasi et al. 2006; Fabrizi et al. 2011) in Italy and the Vallcebre landslide (Corominas et al. 2005) and the Portalet landslide (Herrera et al. 2009; Fernández-Merodo et al. 2014) in Spain.

These case studies concern some landslides having a high value of the length-thickness ratio. Soil deformations occur in a distinct shear zone located at the base of the unstable soil mass that moves with a displacement profile essentially constant with depth. In addition, an evident synchronism was observed between rain and groundwater fluctuations. All these evidences are consistent with the assumptions on which the present method is based.

Location and thickness of the shear zone are established from some inclinometer profiles which also document the progress of the landslide displacement with time. In addition, groundwater level measurements are available for a sufficiently long period of observation. These monitoring data along with the calibration procedure described in the previous section are used to evaluate the model parameters that cannot be found in the above-cited publications. In this connection, it is assumed that the deepest groundwater level recorded in the observation period defines the steady-state level indicated in Fig. 1. In addition, for each case study examined, a borehole (generally located in the central part of the slope) is considered to be representative of the whole landslide body, in accordance with the infinite slope assumption. The results are presented in terms of groundwater level variations, pore water pressure changes at the failure surface, and landslide displacement with time.

The Fosso San Martino landslide

The Fosso San Martino landslide is located near the city of Teramo, in central Italy. It is an active slide which is periodically mobilized by groundwater fluctuations (Bertini et al. 1984; Bertini et al. 1986). A geological cross-section of the slope is shown in Fig. 4. As can be seen, the subsoil essentially consists of a marly clay formation covered by a layer of clayey silt (colluvial cover) with a maximum thickness of about 20 m. The shear zone is located within a layer of weathered marly clay which is interposed between the colluvial cover and the marly clay formation. Figure 5 shows a displacement profile measured at the inclinometer B which is installed in the central part of the slope (Fig. 4). This profile reveals that the soil mass essentially moves like a rigid body sliding over a shear zone, the thickness of which is about 2 m. The piezometric levels recorded at cell B3 are considered to describe the groundwater fluctuations and to define the position of the steady-state groundwater level. This cell is located close to inclinometer B at a depth of 5 m from the ground surface (Fig. 4). On the basis of these data, the slope is modeled as an infinite slope with $H = 22$ m, $H_d = 3.1$ m, and $\alpha = 10°$ (Fig. 1). The available geotechnical parameters which are of interest for the present study are $\gamma = 21$ kN/m^3, $c_r' = 0$ kPa, $\phi_r' = 17°$, and $c_v = 25$ m^2/day (Bertini et al. 1984; Conte and Troncone 2012a). The other parameters are evaluated by matching the available monitoring data with the theoretical results obtained using the proposed method. Specifically, the piezometric measurements carried out at cell B3 from November 1980 to January 1986 along with the monthly rainfall recorded in the same period (Fig. 6a) are first considered to establish the optimum values of $\overline{h}$, k_T, n, and S_r using the calibration procedure described in a precedent section. Then, the time-displacement curve measured at the top of the inclinometer B is considered to estimate the value of β. The values of these parameters are indicated in Table 1. The resulting value of $\overline{h}$ is practically equal to the maximum depth of rain (i.e., rain totally infiltrates into the slope). Figure 6b shows a comparison between the groundwater level variations recorded at cell B3 with those obtained theoretically using Eq. (6) along with the parameters resulting from calibration. In spite of the simplified assumptions made, Eq. (6) reliably predicts the water table depth evolution measured by the piezometer. The mean ($\mu_{residuals}$) and the standard deviation ($\sigma_{residuals}$) of the difference between observations and predictions over the entire record are −0.018 and 0.567 m, respectively. For the sake of completeness, the pore water pressure changes calculated at the failure surface and the value of u_c are shown in Fig. 6c. Comparison in terms of landslide displacement in the horizontal direction (i.e., $s(t)\cos\alpha$) versus time is documented in Fig. 6d. The theoretical results shown in this figure were

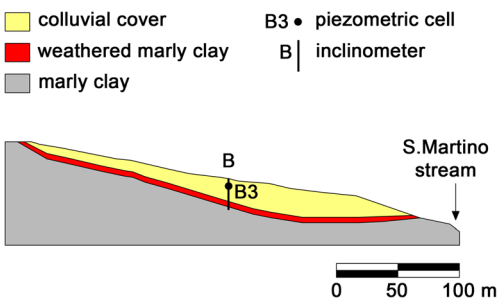

Fig. 4 Fosso San Martino landslide: geological cross-section with an indication of the position of inclinometer B and piezometric cell B3 (modified from Bertini et al. 1986). The scale is applicable to the vertical and horizontal directions

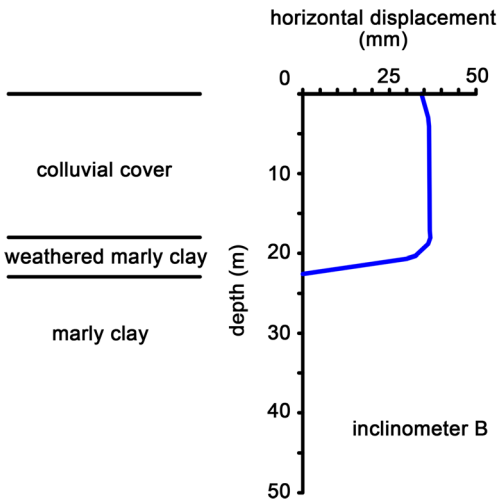

Fig. 5 Fosso San Martino landslide: horizontal displacement profile at inclinometer B (modified from Bertini et al. 1986)

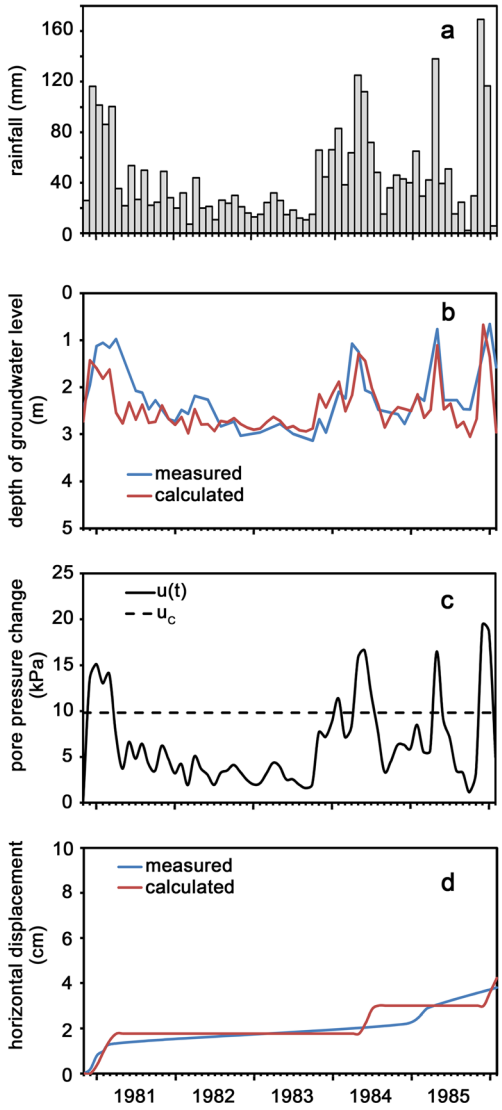

Fig. 6 Fosso San Martino landslide: **a** monthly rainfall; **b** measured and calculated groundwater level changes at cell B3; **c** calculated pore pressure change at the failure surface with an indication of the value of u_c; **d** measured and calculated horizontal displacement versus time at the top of inclinometer B. The groundwater level and displacement measurements are drawn from Bertini et al. (1986)

obtained using the function $u_o(t)$ evaluated theoretically by Eqs. (6) and (7). As can be seen, the global trend of the horizontal displacement is well captured by the method (the values of $\mu_{residuals}$ and $\sigma_{residuals}$ are both equal to 0.009 cm).

The Orvieto landslide

The town of Orvieto is located in central Italy, 105 km north of Rome. It extends on the top of an isolated hill of pyroclastic rock

Table 1 Fosso San Martino landslide: calibrated values of the input parameters

k_T month^{-1}	Porosity (n)	S_r	c_v (m^2/month)	β (kN month/m^3)
20	0.35	0.8	750	6×10^8

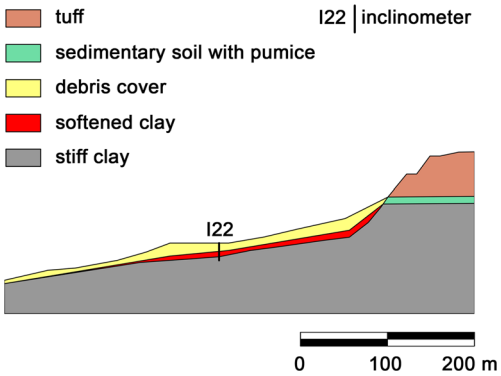

Fig. 7 Orvieto landslide: geological cross-section with an indication of the position of inclinometer I22 (modified from Fabrizi et al. 2011). The scale is applicable to the vertical and horizontal directions

(tuff). The northern slope of this hill is affected by a landslide of great dimensions (the Porta Cassia slide) which continuously causes injuries to some important infrastructures located in that area (Tommasi et al. 2006; Fabrizi et al. 2011). The slope extends over a length of 400 m with an average value of a approximately 7°. As shown in Fig. 7, the subsoil is formed by a stiff clay formation underlying a debris cover that consists of remolded volcanic and clayey materials. The maximum thickness of this cover is about 15 m. The slip surface develops within a softened clay layer with a thickness from 2 to 7 m, which is located at the base of the debris cover (Fig. 8). The residual strength parameters are $c_r' = 0$ kPa and $\phi_r' = 11.3°$, and the average value of the unit weight of the soil is $\gamma = 19.7$ kN/m^3 (Tommasi et al. 1997). For the slope zone where borehole I22 is located (Fig. 7), both inclinometric and piezometric measurements are available for a period from August 2003 to June 2009 (Fabrizi et al. 2011). On the basis of these measurements, it can be assumed that $H = 14.5$ m and $H_d = 3.8$ m. In addition, these measurements, along with the monthly rainfall recorded in the above-specified period (Fig. 9a), are considered in this study to evaluate the other parameters required by the proposed method. The values of the parameters that provided the best agreement between experimental and theoretical results are indicated in Table 2. Figure 9b and d show some comparisons between observation and prediction in terms of

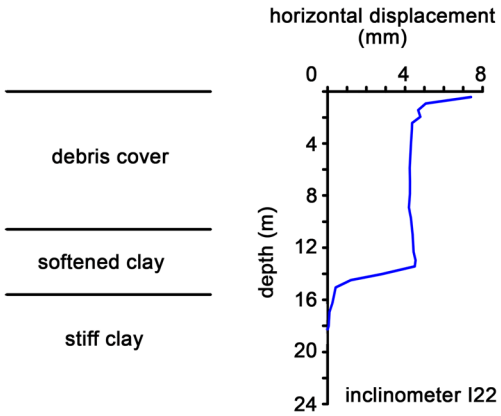

Fig. 8 Orvieto landslide: horizontal displacement profile at inclinometer I22 (modified from Fabrizi et al. 2011)

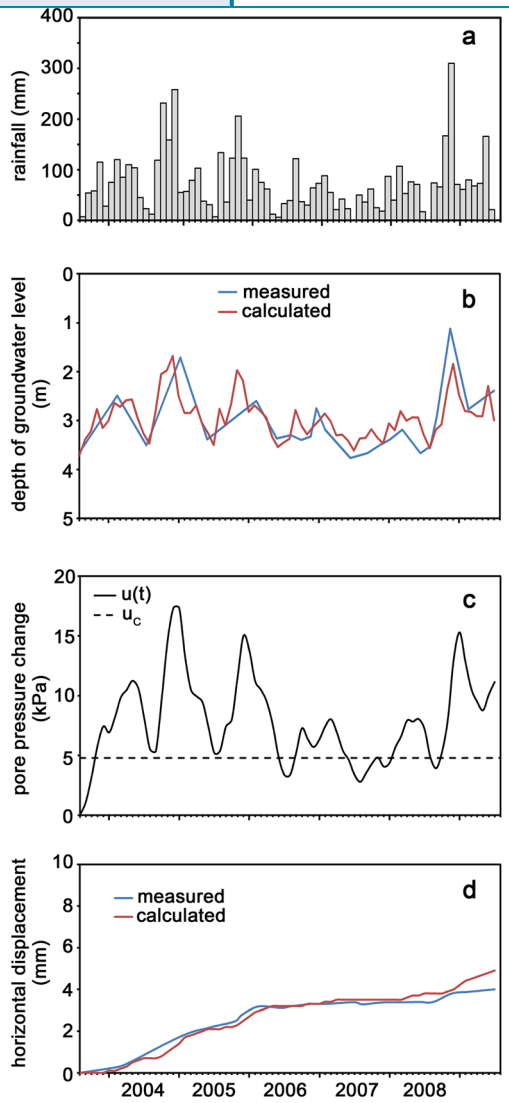

Fig. 9 Orvieto landslide: **a** monthly rainfall; **b** measured and calculated groundwater level changes; **c** calculated pore pressure change at the failure surface with an indication of the value of u_c; **d** measured and calculated horizontal displacement versus time at the top of inclinometer I22. The groundwater level and displacement measurements are drawn from Fabrizi et al. (2011)

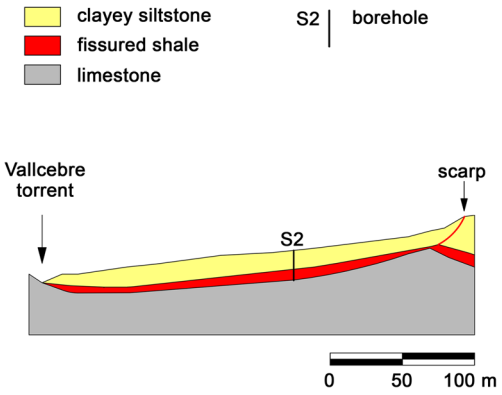

Fig. 10 Vallcebre landslide: geological cross-section with an indication of the position of borehole S2 (modified from Corominas et al. 2005). The scale is applicable to the vertical and horizontal directions

groundwater level changes and horizontal displacement evolution with time, respectively. As can be seen, the proposed approach is able to reproduce reliably the main features of the slope response to rainfall. There is in fact a fairly good agreement between observation and prediction both in terms of rainfall-induced groundwater level variations (Fig. 9b) and in terms of landslide mobility (Fig. 9d). The values of $\mu_{residuals}$ and $\sigma_{residuals}$ concerning the piezometric level variations are 0.102 and 0.340 m, respectively, whereas values of $\mu_{residuals} = -0.002$ mm and $\sigma_{residuals} = 0.0008$ mm are obtained for the residuals of the horizontal displacements. Finally, Fig. 9c shows the pore water pressure changes calculated at the failure surface along with the value of u_c.

The Vallcebre landslide

The Vallcebre landslide is a translational slide located in the Eastern Pyrenees, in Spain (Corominas et al. 2005). The subsoil consists of a thick layer of clayey siltstone with inclusions of gypsum and fissured shale resting on a formation of limestone (Fig. 10). Gypsum is affected by solution processes which cause the formation of fissures, cracks, and vertical holes (pipes). A layer of fissured shale is interposed between the clayey siltstone layer and the limestone formation. The maximum thickness of this latter layer is about 6 m. A complete description of the site from a geological viewpoint can be found in Corominas et al. (2005). The Vallcebre landslide was monitored by installing a significant number of piezometers, inclinometers, and wire extensometers. Since November 1996, systematic measurements of groundwater level and displacement were performed. The monitoring data showed that there is an evident synchronism among rainfall, groundwater fluctuations, and displacement rate (Corominas et al. 2005). This should be ascribed to the presence of fissures, cracks, and pipes that are preferential ways for water infiltration. Inclinometer readings showed that the moving soil mass has a maximum thickness of about 15 m, with deformation concentrated within a shear zone located in the fissured shale layer (Corominas et al. 1999). By contrast, deformation is negligible in the upper layer of clayey siltstone (Fig. 11). In addition, except for the extremities of the landslide body, the shear zone is practically parallel to the ground surface with an average inclination of about 10° (Fig. 10). Referring to Fig. 1, it can be assumed that $H = 15$ m, $H_d = 6.3$ m, and $\alpha = 10°$. The available geotechnical parameters are $\gamma = 21$ kN/m^3, $c_r' = 0$ kPa, $\phi_r' = 13.7°$, and $c_v = 5$ m^2/day (Corominas et al. 2005; Conte and Troncone 2011). Daily rainfall

Table 2 Orvieto landslide: calibrated values of the input parameters

$\overline{h}$ (mm)	K_T month^{-1}	Porosity (n)	S_r	c_v (m^2/month)	β (kN • month/m^3)
200	7	0.6	0.75	50	2.6×10^{10}

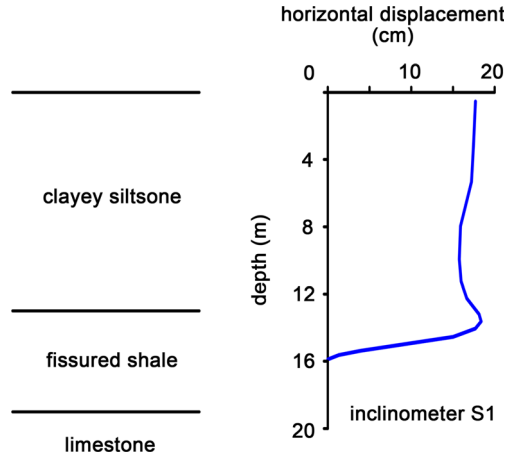

Fig. 11 Vallcebre landslide: horizontal displacement profile at inclinometer S1 (modified from Corominas et al. 1999)

recordings (Fig. 12a) along with groundwater level (Fig. 12b) and ground displacement (Fig. 12d) measurements at the borehole S2 (Fig. 10) are considered in this study to evaluate the other required parameters using the calibration procedure described in the precedent section. The best agreement between measured and calculated results is achieved using the values shown in Table 3. Figure 12b presents a comparison between the piezometric levels recorded from March 1997 to February 1998 and those predicted by Eq. 6. The values of $\mu_{residuals}$ and $\sigma_{residuals}$ are 0.322 and 0.877 m, respectively. They are greater than those found for the other case studies considered in the present paper. This worse fitting should be principally ascribed to the presence of two peaks in the calculated function $h(t)$, which are consistent with the rainfall record (Fig. 12a), but not with the groundwater level measurements (Fig. 12b). In addition, Fig. 12c shows the pore water pressure changes calculated at the failure surface, and Fig. 12d compares the accumulated displacement measured at the top of borehole S2 with those calculated using the present method. Referring to the latter comparison, the calculated values of $\mu_{residuals}$ and $\sigma_{residuals}$ are 0.005 and 0.020 cm, respectively. Therefore, the agreement between observed and calculated landslide displacements can be considered satisfactory.

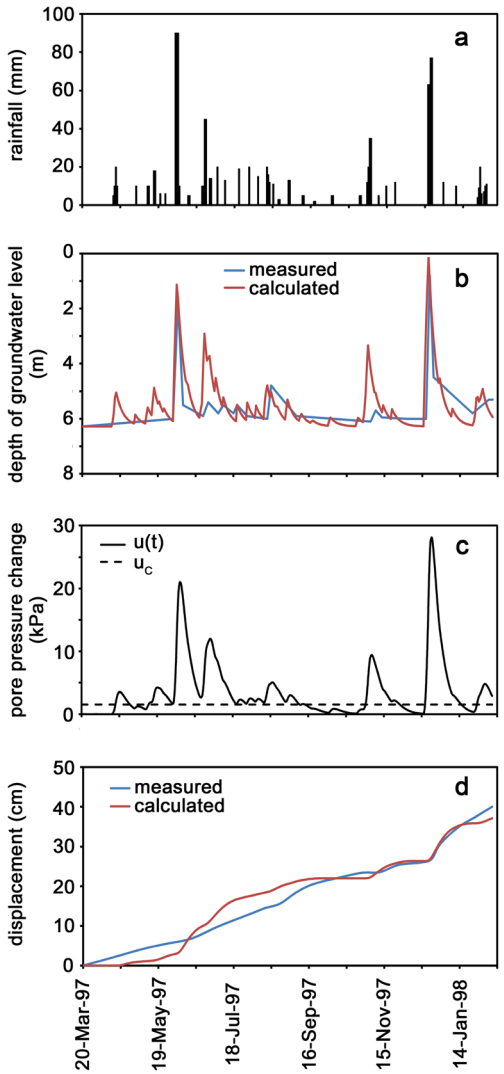

Fig. 12 Vallcebre landslide: **a** daily rainfall; **b** measured and calculated groundwater level changes; **c** calculated pore pressure change at the failure surface with an indication of the value of u_c; **d** measured and calculated displacement versus time at the top of borehole S2. The groundwater level and displacement measurements are drawn from Corominas et al. (2005)

The Portalet landslide

The study area is located in the central Spanish Pyrenees and is affected by several landslides. The landslide considered in the present study is a paleolandslide that was reactivated owing to the construction of a parking area at the toe of the slope (Herrera et al. 2009). As shown in Fig. 13, the subsoil is characterized by the presence of a slate formation covered by three different soil layers (Fernández-Merodo et al. 2014). The shallowest layer is formed by a colluvial deposit (up to 10 m thick) consisting of gravel, sand, and sandy clayey silt with limestone boulders. Below this deposit, a layer of silt and sandy clay is present. The third layer is made up of fractured and weathered slate. The slope model considered in the present analysis is based on the experimental data from the borehole S-1, the location of which is indicated in Fig. 13. Readings at the inclinometer installed in this borehole show that the slip surface is located at a depth of approximately 13.5 m from the slope surface (Fig. 14). Displacement measurements at several control points located on the ground surface were also performed using SAR and DGPS monitoring techniques. The respective results are described in details by Herrera et al. (2009); Fernández-Merodo et al. (2014). On the basis of these data, it can be assumed that $H = 13.5$ m and $\alpha = 14°$ (Fig. 1). In addition, the following geotechnical parameters are available: $\gamma = 22.7$ kN/m^3, $n = 0.15$, $c_r' = 0$ kPa, and $\phi_r' = 18°$ (Herrera et al. 2009). In particular, the values of c_r' and ϕ_r' define the residual strength of the silt and sandy clay layer where the shear zone is located (Fig. 14). In situ measurements carried out at some piezometers in the period from July 2010 to October 2011 show that the steady-state groundwater level is 6.5 m deep and that its changes with time are strongly influenced by rainfall (Fig. 15a, b). Such a close relationship between rainfall and groundwater fluctuations should be ascribed to the drainage capacity of the upper layer of colluvium and the presence of superficial cracks and preferential drainage pathways (Fernández-Merodo et al. 2014). The parameters

Table 3 Vallcebre landslide: calibrated values of the input parameters

$\overline{h}$ (mm)	k_T day^{-1}	Porosity (n)	S_r	c_v (m^2/day)	β (kN • day/m^3)
60	1	0.3	0.9	5	1×10^8

used in the calculations are those specified above in addition to those indicated in Table 4. Considering the value found for $\overline{h}$ (i.e., 90 mm), it can be assumed that rain totally infiltrates into the slope (Fig. 15a). It is also noteworthy that the parameters c_v and β were evaluated on a trial-and-error basis, because of the few displacement measurements available (Fernández-Merodo et al. 2014). A comparison between observed and predicted groundwater levels is shown in Fig. 15b ($\mu_{residuals}$ and $\sigma_{residuals}$ are 0.076 and 0.438 m, respectively). Function $u_o(t)$ obtained from Eq. (7) is used as input for calculating the pore water pressure changes at the failure surface (Fig. 15c) and the horizontal displacement evolution with time. Finally, Fig. 15d presents a comparison between the calculated displacements and those measured at the ground surface. From the comparisons documented in Fig. 15b, d, it can be concluded that the theoretical results approximate the available measurements well, both in terms of groundwater level fluctuations and horizontal displacements.

Discussion and conclusions

Active landslides are often controlled by the groundwater level fluctuations which in turn are related to rainfall. These landslides are generally characterized by low velocity with deformations essentially concentrated within a distinct shear zone located at the base of the landslide body (Leroueil et al. 1996). The soil mass above the shear zone is, on the contrary, affected by small deformations and moves like a rigid body (i.e., with a horizontal displacement profile that is essentially constant with depth). Movements are usually generated by a rise in groundwater level owing to rainfall. On the other hand, a drop in groundwater reduces the landslide velocity until the unstable soil mass comes to rest. Therefore, the mobility of these landslides is marked by alternating phases of rest and motion.

In view of these evidences, a method based on a simple sliding block model has been presented in this study for a preliminary evaluation of the landslide mobility in relation to rainfall. The proposed method can be applied to landslides that exhibit a direct coupling between precipitation and groundwater levels, for example, owing to the presence of ground fissures, cracks, and preferential drainage pathways which favor water infiltration into the slope (Van Asch et al. 1996). Therefore, the method is unsuitable for analyzing study cases showing a complex relationship among rainfall, groundwater levels, and displacements (Novotný and Kobr 2009). In these circumstances, the method only provides a first approximation of the slope response to rainfall.

Several methods based on the sliding block model were previously published in the literature (Hutchinson 1986; Angeli et al. 1996; Gottardi and Butterfield 2001; Corominas et al. 2005; Herrera et al. 2009; Ranalli et al. 2010; Conte and Troncone 2011, 2012c). In these methods, however, the landslide movements are calculated using, as input data, the groundwater level measurements performed at some piezometers installed within the slope. This constitutes a serious drawback when such methods are used to predict displacement scenarios from expected rainfall scenarios, because the groundwater level changes associated with precipitation are not known. Unlike the abovementioned methods, the present approach directly relates landslide movements to rain recordings. Specifically, the proposed method utilizes some novel equations that relate rainfall to groundwater level changes and the latter to the landslide movements. Field measurements of groundwater level and landslide displacement are however necessary to evaluate some parameters that are difficult to evaluate experimentally. In particular, the parameters k_T and β should be carefully selected because they significantly affect the prediction of the groundwater level changes and landslide movements, respectively. To this purpose, an optimization procedure has also been incorporated in the proposed method. After performing the parameter calibration, the

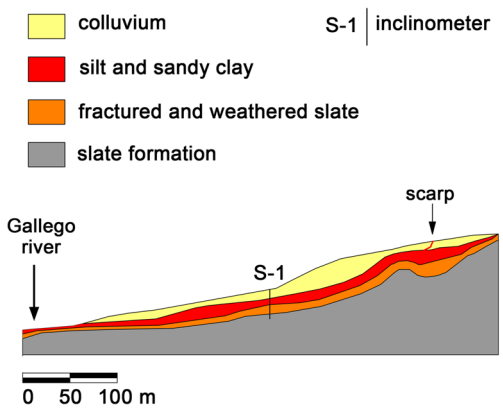

Fig. 13 Portalet landslide: geological cross-section with an indication of the position of inclinometer S-1 (modified from Fernández-Merodo et al. 2014). The scale is applicable to the vertical and horizontal directions

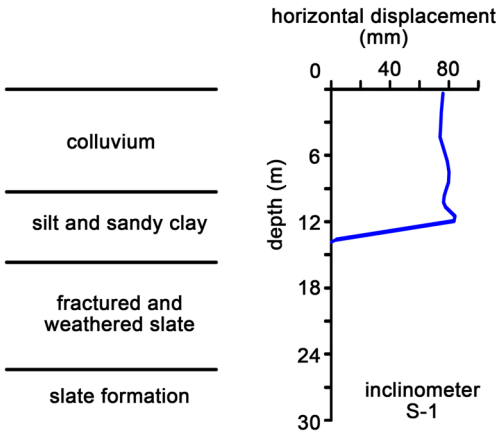

Fig. 14 Portalet landslide: horizontal displacement profile at inclinometer S-1 (modified from Fernández-Merodo et al. 2014)

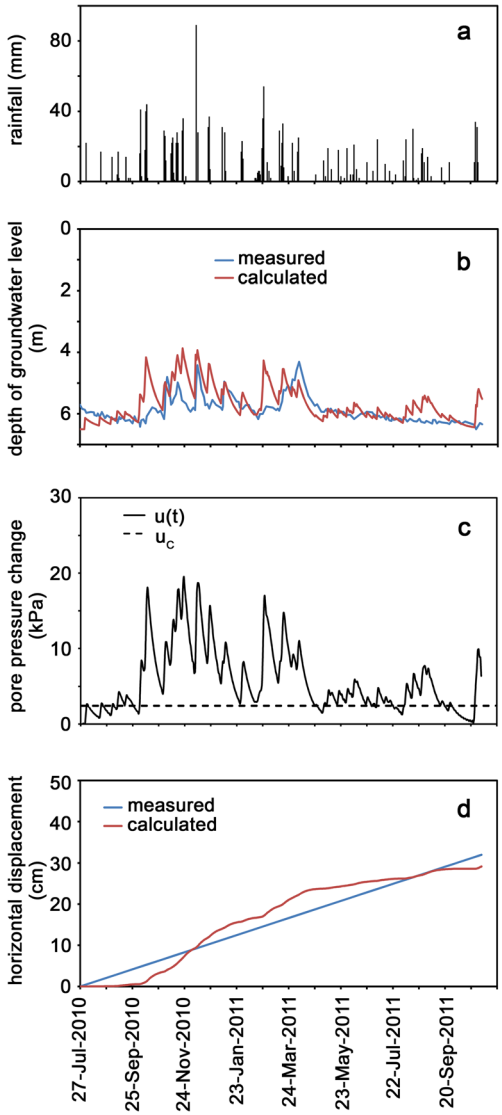

Fig. 15 Portalet landslide: **a** daily rainfall; **b** measured and calculated groundwater level changes; **c** calculated pore pressure change at the failure surface with an indication of the value of u_c; **d** measured and calculated horizontal displacement versus time at the top of inclinometer S-1. The groundwater level and displacement measurements are drawn from Fernández-Merodo et al. (2014)

method may be used for planning and construction purposes, to predict future landslide movements directly from expected rain events. Considering that the present method is in principle able to analyze landslides with different degrees of mobility, a further application could concern the definition of rainfall thresholds for slow and fast landslides. This subject will be dealt with in a future study.

Four case studies documented in the literature have been considered in order to assess the capability of the present method to reproduce the main features of the landslide response to rainfall. For the sake of generality, two cases concern landslides with slow movement and the others concern landslides that move more quickly. In all these case studies, an evident synchronism subsists between rain and groundwater fluctuations (as required by Eqs. 1a to 6) owing to the presence of ground fissures and preferential ways for water infiltration. In addition, the landslide bodies at issue have a length much greater than the thickness, and soil deformations essentially occur in a shear zone located at the base of the moving soil mass, in line with the assumption of infinite slope and sliding rigid block, respectively. As a consequence, the proposed approach should be suitable for analyzing the case studies considered. To this regard, statistics of the difference between measurements and predictions have proved that both groundwater level variations and landslide displacements observed in field are well approximated by the present method. The method should also be of significant interest from a practical viewpoint when there is a lack of specific experimental data. In these circumstances, in fact, the use of more sophisticated and computationally costly methods (Olivella et al. 1996; Picarelli et al. 2004; Fernández-Merodo et al. 2014; Conte et al. 2014) could not be completely justified.

Table 4 Portalet landslide: calibrated values of the input parameters

k_T day^{-1}	S_r	c_v (m^2/day)	β (kN • day/m^3)
0.3	0.6	20	8×10^9

References

Angeli MG, Gasparetto P, Menotti RM, Pasuto A, Silvano S (1996) A visco-plastic model for slope analysis applied to a mudslide in Cortina d'Ampezzo, Italy. Q J Eng Geol 29(3):233–240

Bertini T, D'Elia B, Grisolia M, Olivero S, Rossi-Doria M (1984) Climatic conditions and slow movements of colluvium covers in central Italy. In: Proceedings 4th International Symposium on Landslides, Toronto, vol. 1, pp 367–376

Bertini T, Cugusi F, D'Elia B, Rossi-Doria M (1986) Lenti movimenti di versante nell'Abruzzo adriatico: caratteri e criteri di stabilizzazione. In: Proceedings 16th Convegno Nazionale di Geotecnica, Bologna, AGI, Roma, vol. 1, pp 91–100

Bracegirdle A, Vaughan PR, High DW (1992) Displacement prediction using rate effects on residual shear strength. In: Proceedings 6th International Symposium on Landslides, Christchurch, New Zealand, vol. 1, pp 343–348

Calvello M, Cascini L, Sorbino G (2008) A numerical procedure for predicting rainfall-induced movements of active landslides along pre-existing slip surfaces. Int J Numer Anal Methods Geomech 32(4):327–351

Coleman TF, Li Y (1994) On the convergence of reflective newton methods for large-scale nonlinear minimization subject to bounds. Math Program 67(2):189–224

Coleman TF, Li Y (1996) An interior, trust region approach for nonlinear minimization subject to bounds. SIAM J Optim 6:418–445

Conte E, Troncone A (2008) Soil layer response to pore pressure variations at the boundary. Geotechnique 58(1):37–44

Conte E, Troncone A (2011) An analytical method for predicting the mobility of slow-moving landslides owing to groundwater fluctuations. J Geotech Geoenviron Eng ASCE 137(8):777–784

Conte E, Troncone A (2012a) Stability analysis of infinite clayey slopes subjected to pore pressure changes. Geotechnique 62(1):87–91

Conte E, Troncone A (2012b) A method for the analysis of soil slips triggered by rainfall. Geotechnique 62(3):187–192

Conte E, Troncone A (2012c) Simplified approach for the analysis of rainfall-induced landslides. J Geotech Geoenviron Eng ASCE 138(3):398–406

Conte E, Donato A, Troncone A (2014) A finite element approach for the analysis of active slow-moving landslides. Landslides 11(4):723–731

Corominas J, Moya J, Ledesma A, Rius JA, Gili JA, Lloret A (1999) Monitoring of the Vallcebre landslide, Eastern Pyrenees, Spain. In: Proceedings International Symposium on Slope Stability Engineering, Shikoku, Japan, pp 1239–1244

Corominas J, Moya J, Ledesma A, Lloret A, Gili JA (2005) Prediction of ground displacements and velocities from groundwater level changes at the Vallcebre landslide (Eastern Pyrenees, Spain). Landslides 2(2):83–96

Cruden DM, Varnes DJ (1996) Landslides—investigation and mitigation. Special report No. 247, transportation research board. National Academy Press, Washington
Desai CS, Samtani NC, Vulliet L (1995) Constitutive modeling and analysis of creeping soils. J Geotech Eng ASCE 121(1):43–56
Di Maio C, Vassallo R, Vallario M, Pascale S, Sdao F (2010) Structure and kinematics of a landslide in a complex clayey formation of the Italian Southern Apennines. Eng Geol 116(3–4):311–322
Fabrizi O, Barba M, Forbicioni R, Grifoni M, Massi S (2011) Monitoraggio delle aree in frana della rupe di Orvieto: rete inclinometrica e piezometrica a lettura manuale. Int. Report, Servizio Geologico e Sismico Regione Umbria, Perugia
Fernández-Merodo JA, García-Davalillo JC, Herrera G, Mira P, Pastor M (2014) 2D viscoplastic finite element modelling of slow landslides: the Portalet case study (Spain). Landslides 11(1):29–42
Gottardi G, Butterfield R (2001) Modelling 10 years of downhill creep data. In: Proceedings 5th International Conference on Soil Mechanics and Geotechnical Engineering, Istanbul, Turkey, vol. 1–3, pp 27–31
Herrera G, Fernández-Merodo JA, Mulas J, Pastor M, Luzi G, Monserrat OA (2009) Landslide forecasting model using ground based SAR data: the Portalet case study. Eng Geol 105(3–4):220–230
Hutchinson JN (1986) A sliding-consolidation model for flow slides. Can Geotech J 23:115–126
Leroueil S, Vaunat J, Picarelli L, Locat J, Faure R, Lee H (1996) A geotechnical characterization of slope movements. In: Proceedings 7th International Symposium on Landslides, Trondheim, vol. 1, pp 53–74
Lollino P, Elia G, Cotecchia F, Mitaritonna G (2010) Analysis of landslide reactivation mechanisms in Daunia clay slopes by means of limit equilibrium and FEM methods. Geotech Spec Publ 199:3155–3164
MathWorks (2012) Matlab user's guide. The MathWorks Inc, Natick
Montrasio L, Valentino R (2007) Experimental analysis and modelling of shallow landslides. Landslides 4(3):291–296
Montrasio L, Valentino R (2008) A model for triggering mechanisms of shallow landslides. Nat Hazards Earth Syst Sci 8:1149–1159
Novotný J, Kobr M (2009) Hydrogeological pattern of groundwater flow of landslides in cretaceous claystones based on long-term groundwater monitoring and hydrologging measurement. Environ Geol 58(1):25–32
Olivella S, Gens A, Carrera J, Alonso EE (1996) Numerical formulation for a simulator (CODE_BRIGHT) for the coupled analysis of saline media. Eng Comput 13:87–112
Picarelli L, Urciuoli G, Russo C (2004) Effect of groundwater regime on the behaviour of clayey slopes. Can Geotech J 41:467–484
Ranalli M, Gottardi G, Medina-Cetina Z, Nadim F (2010) Uncertainty quantification in the calibration of a dynamic viscoplastic model of slow slope movements. Landslides 7(1):31–41
Savage WZ, Chleborad AF (1982) A model for creeping flow in landslides. Bull Assoc Eng Geol 19(4):333–338
Tommasi P, Ribacchi R, Sciotti M (1997) Slow movements along the slip surface of the 1900 Porta cassia landslide in the clayey slope of the orvieto hill. Rivista Italiana di Geotecnica 31(2):49–58
Tommasi P, Pellegrini P, Boldini D, Ribacchi R (2006) Influence of rainfall regime on hydraulic conditions and movement rates in the overconsolidated clayey of the Orvieto hill (central Italy). Can Geotech J 43:70–86
Van Asch TWJ, Buma JT (1997) Modelling groundwater fluctuations and the frequency of movement of a landslide in the terres noires region of barcelonnette (France). Earth Surf Process Landf 22:131–141
Van Asch TWJ, Van Genuchten PMB (1990) A comparison between theoretical and measured creep profiles of landslides. Geomorphology 3:45–55
Van Asch TWJ, Hendriks MR, Hessel R, Rappange FE (1996) Hydrological triggering conditions of landslides in varved clays in the French Alps. Eng Geol 42:239–251
Van Asch TWJ, Van Beek LPH, Bogaard TA (2007) Problems in predicting the mobility of slow-moving landslides. Eng Geol 91:46–55
Vassallo R, Grimaldi GM, Di Maio C (2015) Analysis of transient pore pressure distribution and safety factor of a slow clayey deep-seated landslide by 2D and 3D models. Engineering geology for society and territory, vol 2. Springer, Berlin
Vulliet L, Hutter K (1988) Viscous-type sliding laws for landslides. Can Geotech J 25(3):467–477

E. Conte · A. Donato · A. Troncone (✉)
Department of Civil Engineering,
University of Calabria,
Via P. Bucci, Cubo 44/b, 87036, Rende, Cosenza, Italy
e-mail: antonello.troncone@unical.it

E. Conte
e-mail: enrico.conte@unical.it
e-mail: antonio.donato@unical.it